Juan Ji An, Yumie Rhee, Se Hwa Kim, Dol
Mi Kim, Dong-He Han, Jung Hee Hwang,
Young-Jun Jin, Bong Soo Cha, Ja-Hyun Baik,
Won Tae Lee and Sung-Kil Lim

Access the most updated version of this article at doi: 10.1074/jbc.M603454200

Find articles, minireviews, Reflections and Classics on similar topics on the JBC Affinity Sites.

Alerts:

- When this article is cited
- When a correction for this article is posted

Click here to choose from all of JBC's e-mail alerts

Supplemental material:

http://www.jbc.org/content/suppl/2006/11/24/M603454200.DC1.html

This article cites 50 references, 18 of which can be accessed free at
http://www.jbc.org/content/282/5/2862.full.html#ref-list-1

Peripheral Effect of α-Melanocyte-stimulating Hormone on Fatty Acid Oxidation in Skeletal Muscle*□S

Juan Ji An[‡§¶], Yumie Rhee[‡], Se Hwa Kim[‡], Dol Mi Kim[‡], Dong-He Han[‡§], Jung Hee Hwang[‡§], Young-Jun Jin[∥], Bong Soo Cha[‡], Ja-Hyun Baik[**], Won Tae Lee[‡‡], and Sung-Kil Lim[‡§1]

From the ‡Department of Internal Medicine & Endocrine Research Institute, §Brain Korea 21 Project for Medical Sciences, Yonsei University College of Medicine, 134 Shinchon-Dong, Seodaemoon-Gu, Seoul 120-752, Korea, the ¶Division of Endocrinology, Department of Internal Medicine, Affiliated Hospital, Medical College, Yanbian University, Yanji 133000, People's Republic of China, the ∥Division of Endocrinology, Department of Internal Medicine, Affiliated Hospital of Binzhou Medical College, Shanbong 256600, People's Republic of China, the **School of Life Sciences and Biotechnology, Korea University, Seoul 136-713, Korea, and the ‡‡Department of Biochemistry, Yonsei University, Seoul 120-749, Korea

To study the peripheral effects of melanocortin on fuel homeostasis in skeletal muscle, we assessed palmitate oxidation and AMP kinase activity in α-melanocyte-stimulating hormone (α-MSH)-treated muscle cells. After α-MSH treatment, carnitine palmitoyltransferase-1 and fatty acid oxidation (FAO) increased in a dose-dependent manner. A strong melanocortin agonist, NDP-MSH, also stimulated FAO in primary culture muscle cells and C2C12 cells. However, [Glu⁶]α-MSH-ND, which has ample MC4R and MC3R agonistic activity, stimulated FAO only at high concentrations (10^{-5} M). JKC-363, a selective MC4R antagonist, did not suppress α-MSH-induced FAO. Meanwhile, SHU9119, which has both antagonistic activity on MC3R and MC4R and agonistic activity on both MC1R and MC5R, increased the effect of α-MSH on FAO in both C2C12 and primary muscle cells. Small interference RNA against MC5R suppressed the α-MSH-induced FAO effectively. cAMP analogues mimicked the effect of α-MSH on FAO, and the effects of both α-MSH and cAMP analogue-mediated FAO were antagonized by a protein kinase A inhibitor (H89) and a cAMP antagonist ((R_p)-cAMP). Acetyl-CoA carboxylase activity was suppressed by α-MSH and cAMP analogues by phosphorylation through AMP-activated protein kinase activation in C2C12 cells. Taken together, these results suggest that α-MSH increases FAO in skeletal muscle, in which MC5R may play a major role. Furthermore, these results suggest that α-MSH-induced FAO involves cAMP-protein kinase A-mediated AMP-activated protein kinase activation.

Obesity is a major health problem in humans; it is associated with an increased risk of type 2 diabetes, as well as with cardiovascular and cerebrovascular diseases. Impaired cellular metabolism in target tissues that regulate fuel homeostasis is one of the pathogenic factors associated with obesity and type 2 diabetes (1). Skeletal muscle plays a major role in determining whole body energy expenditure. In humans, skeletal muscle accounts for >70% of the body's total glucose disposal (2). Recent studies utilizing computerized tomography and magnetic resonance imaging have demonstrated that adipose tissue located beneath the fascia lata is metabolically important in obesity and type 2 diabetes (3, 4). The amount of triglycerides in skeletal muscle, although quite small relative to that in adipose tissue, is closely associated with insulin resistance (4–6).

The central melanocortin system is important in the control of food intake and body weight. Proopiomelanocortin neurons in the hypothalamus mediate leptin-induced catabolic effects (7). The importance of the melanocortin pathway in the regulation of energy homeostasis has been elucidated using pharmacological and genetic evidence (8, 10–14). α-Melanocyte-stimulating hormone (α-MSH)[2] and its analogues acutely suppress food intake after intracerebroventricular administration in rats and mice (8, 9). Moreover, genetic disruption of MC4R has been found to cause obesity in mice (10). Recent experiments in MC3R knock-out mice indicate that inactivation of MC3R results in increased fat mass and reduced body mass, despite the fact that the animals were hypophagic and maintained normal metabolic rates (11, 12). However, the peripheral effects of melanocortins have not been extensively studied, even though α-MSH has been shown to have direct effects on several peripheral organ systems (13, 15). Among the five subtypes of MCRs, MC5R is the predominant subtype expressed in skeletal muscle (16), suggesting a direct peripheral action for melanocortins in this tissue. Recently, the role of melanocortins and MCRs in adipocytes has been studied (17–19). However, the effects of melanocortins on skeletal muscle are not well understood.

It has been postulated that fatty acid oxidation (FAO) in skeletal muscle is regulated in part by malonyl-CoA. Malonyl-CoA is an inhibitor of carnitine palmitoyltransferase-1 (CPT-1), which controls the transfer of long-chain fatty acyl-CoA mole-

2 The abbreviations used are: α-MSH, α-melanocyte-stimulating hormone; MCR, melanocortin receptor; FAO, fatty acid oxidation; AMPK, AMP-activated protein kinase; CPT-1, carnityl palmitoyl transferase-1; ACC, acetyl-CoA carboxylase; siRNA, small interfering RNA; Bt₂cAMP, dibutyryl cAMP; PKA, protein kinase A; RT, reverse transcription; NDP, norleucine-D-phenylalanine; ND, norleucine-D.

cules into the mitochondria for oxidation (20, 21). Malonyl-CoA is synthesized from cytosolic acetyl-CoA through a reaction catalyzed by acetyl-CoA carboxylase (ACC). Meanwhile, AMP-activated protein kinase (AMPK) is a fuel-sensing enzyme present in most mammalian tissues (22). In exercising skeletal muscle, activation of AMPK increased glucose transport (23) and FAO (22, 24) through the inhibition of ACC and activation of malonyl-CoA decarboxylase by phosphorylation, leading to a decrease in the concentration of malonyl-CoA and an increase in CPT-1 activity (25). It has been reported that leptin stimulates FAO and glucose uptake and prevents the accumulation of lipids through AMPK activation and ACC inhibition (26). However, whether melanocortins stimulate the oxidation of fatty acid in nonadipose tissues has not yet been determined.

To assess the peripheral regulation of melanocortins on fuel homeostasis in skeletal muscle, we studied 1) the effect of α-MSH analogues on FAO, 2) which MCRs play major roles in mediating FAO, 3) downstream signals after MCR activation, and 4) the role of AMPK in skeletal muscle FAO. Here, we showed that α-MSH regulates FAO through the activation of the MCR-mediated protein kinase A (PKA)-AMPK signal transduction pathway in skeletal muscle.

EXPERIMENTAL PROCEDURES

Materials—α-MSH, NDP-MSH, and [Glu[6]]α-MSH-ND peptides were synthesized at Peptron (Daejon, Korea). L-[*methyl*-^{14}C]Carnitine and [9,10-^{3}H]palmitic acid were obtained from Amersham Biosciences. SHU9119, JKC-363, dibutyryl-cAMP, 8-Br-cAMP, R_p-8-Br-cAMP, and H89 were obtained from Sigma. Anti-phospho-acetyl-CoA polyclonal antibody and Anti-acetyl-CoA polyclonal antibody were obtained from Upstate Co. (Bedford, MA).

Animals—Eight-week-old C57BL/6J male mice were obtained from the Jackson Laboratory (Daehan Biolink Co., Seoul, Korea). Animals were maintained under a 12-h light-dark cycle at 23 °C according to institutional guidelines for the humane treatment of laboratory animals. All experimental protocols were approved by the Animal Ethics Committee of the University of Yonsei, College of Medicine (Seoul, Korea). Mice were housed with free access to food and water and were removed from the cages from 9:00 a.m. to 4:00 p.m. during the experiments.

Myocyte Cell Cultures—A monolayer of mouse C2C12 myoblasts cells were grown in high glucose Dulbecco's modified Eagle's medium (Dulbecco's modified Eagle's medium 90%/10% (v/v) fetal calf serum, Invitrogen) in a humidified incubator at 37 °C containing 5% CO_2. Cells were grown in 100-mm dishes, sub-cultured at 60–80% confluence, and split at a ratio of 1:10 using trypsin-EDTA. Cells grown to 60% confluence were sub-cultured at a ratio of 1:15 into 6-well dishes. When the cells were 80% confluent, differentiation into myoblasts containing myotubes was induced by switching to low serum differentiation medium (98% Dulbecco's modified Eagle's medium and 2% (v/v) horse serum). Differentiation medium was changed daily. By day 6, the cells were fully confluent and had differentiated into multinucleated myoblasts with contracting myotubes.

Primary Muscle Cell Culture—The hind limbs of 3-week-old mouse fetuses were used to prepare muscle cell cultures (27). In brief, muscle tissue was dissected from the hind limbs under a microscope, and the tissue was then minced into small pieces with scissors. The suspension was digested with 0.1% (w/v) collagenase, 0.2% trypsin, and 0.1% DNase at 37 °C for 30 min. Dulbecco's modified Eagle's medium containing 10% fetal calf serum and 10% horse serum (growth medium) was added to the suspension. The remaining tissue fragments were dissociated by triturating with a 10-ml pipette. The cell suspension was centrifuged at 2000 × g for 5 min, and the supernatant was discarded. Twenty microliters of growth medium was added, and the suspension was again triturated with a 10-ml wide-bore pipette to dissociate aggregated cells. The suspension was filtered through a 70-μm nylon mesh, and the cells were seeded onto two 100-mm Petri dishes for 45 min. During this time, the fibroblasts attached to the bottom of the dish, while the myoblasts remained in suspension. The medium was removed and the dishes were discarded. Cells were counted and seeded onto 100-mm dishes coated with 0.1% gelatin. For the purpose of further purification of the myocytes, fibroblasts and other contaminating cell types were removed by dispase treatment 48 h after seeding, as described by Daniels (27). All experiments were performed on first passage cells 11–12 days after re-plating.

RT-PCR Reaction—Total RNA from the hypothalamus, skeletal muscle, liver, pancreas, and C2C12 cells was isolated using Tri reagent (Invitrogen) and treated with DNase I (Promega, Madison, WI). RNA was quantified by measuring absorbance at 260 nm; the A_{260}/A_{280} ratio was 1.8 or higher. One microgram of total RNA was reverse-transcribed using 2 units of Moloney murine leukemia virus reverse transcriptase (Promega), 0.5 μg of random primer (Promega), 0.25 mM dNTPs (Promega), and 10 units of RNasin (Promega) in a final volume of 20 μl. PCR amplification was performed using 1 μl of RT products, 0.2 mM dNTPs, and 1.5 unit of *Taq* polymerase (Promega) in a final volume of 50 μl. PCR amplification for each melanocortin receptor was performed with 35 cycles of 30 s at 94 °C, 30 s at 50 °C, and 1 min at 72 °C. The following oligonucleotides were used for RT-PCR amplification: MC1R: forward, 5′-GCC ACC CTT ACT ATC CTT CT-3′; reverse, 5′-ATA TCA CTG TCA CCC TCT GC-3′; MC3R: forward, 5′-CAAGATGGTCATCG-TGTGTCT-3′; reverse, 5′-TAGCCCAAGTTCATGCTGTT-3′; MC4R: forward, 5′-ATCATTTACTCGGACAGCAGC-3′; reverse, 5′-ACAACTCACAGATGCCTCCCA-3′; MC5R: forward, 5′-TCATTTGCCTCATCTCCATGT-3′; reverse, 5′-ACT-GAGAGAGGAAGGCGTTT-3′; and β-actin: forward, 5′-TTC-AACACCCCAGCCATGT-3′; reverse, 5′-TGTGGTACGA-CCAGAGGCATAC-3′.

Muscle Mitochondria Preparation and CPT-1 Activity Assay—Animals were sacrificed by decapitation. The soleus muscles were homogenized in 0.15 M KCl medium containing 10 mM Tris-HCl (pH 7.4) and 1 mM EDTA. Mitochondria were isolated as described by Saggerson and Carpenter (28) and resuspended in 0.15 M KCl medium. Mitochondrial protein levels were measured using Lowry's method (29). Enzyme activity was determined within 15 min of mitochondrial isolation by measuring the incorporation of L-[*methyl*-^{14}C]carnitine into the *n*-butanol-soluble product (28). Mitochondria (250 μg of protein)

were preincubated at 25 °C for 4 min in 1.0 ml of a mixture containing 150 mM sucrose, 60 mM KCl, 25 mM Tris-HCl (pH 7.4), 1 mM EDTA, 1 mM dithiothreitol, 40 μM palmitoyl-CoA, and 1.3 mg/ml albumin (fatty acid-free). Reactions were started by adding 25 μl of a solution containing 1 μCi (0.4 μmol) of L-[*methyl*-^{14}C]carnitine and continued for up to 4 min. The reactions were then stopped by adding 1.0 ml of ice-cold 1 N HCl. Blank values were determined by replacing the mitochondrial samples with an equal volume of resuspension buffer.

Measurement of Palmitate Oxidation in the Primary Muscle Cells and C2C12 Cells—FAO was measured by quantifying the production of ^{3}H$_2$O from [9,10-^{3}H]palmitate as previously described (30). Briefly, the cells were trypsinized, counted, plated (1×10^6 cells per well in 12-well coated microplates), and allowed to grow for 6 days in differentiation medium. Tritiated water release experiments were performed in triplicate. Cultured muscle cell layers were washed three times with Dulbecco's phosphate-buffered saline. Next, 500 μl of [9,10-^{3}H]palmitic acid (53 Ci/mmol) was bound to fatty acid-free albumin (final concentration: 125 μM, palmitate: albumin = 1:1). α-MSH was added as specified for each experiment. The incubation was carried out for 2 h at 37 °C. After incubation, the mixture was removed and added to a tube containing 200 μl of cold 10% trichloroacetic acid. The tubes were centrifuged for 10 min at 2,200 $\times$ g at 4 °C. Aliquots of the supernatants (350 μl) were removed, mixed with 55 μl of 6 N NaOH, and applied to ion-exchange resin. The columns were washed twice with 750 μl of water, and the eluants were counted.

AMPK Assay—AMPK activity was measured as previously described (31). Differentiated cells on 6-well plates were incubated with the indicated concentrations of ligands for the specified periods at 37 °C. Cell lysates were prepared with a buffer containing 1% Nonidet P-40 and were immunoprecipitated with an anti-AMPKα2-subunit antibody (Upstate) and protein A/G-agarose beads (Santa Cruz Biotechnology, Santa Cruz, CA). The beads were washed three times with washing buffer (20 mM Tris-HCl, pH 8.0, 140 mM NaCl, 1% Nonidet P-40, and 1 mM dithiothreitol) and once with AMPK assay buffer (40 mM HEPES, 200 mM AMP, 80 mM NaCl, 0.8 mM dithiothreitol, 5 mM MgCl$_2$, pH 7.0). The immunoprecipitates were resuspended in 30 μl of assay mixture (40 mM HEPES, 200 mM AMP, 80 mM NaCl, 0.8 mM dithiothreitol, 5 mM MgCl$_2$, 0.2 mM ATP, 0.1 mM "SAMS" peptide, and 2 μCi of [γ-^{32}P]ATP) and incubated for 20 min or the indicated periods at 30 °C. Twenty microliters of the supernatant was spotted onto Whatman P81 chromatography paper. The filter was then washed four times with 1% phosphoric acid and air dried. AMPK activity was determined by measuring the incorporation of ^{32}P using scintillation counting.

Adenoviral Gene Transfer of Dominant-negative $\alpha1$ and $\alpha2$ AMPK—Plasmid encoding c-Myc-tagged forms of dominant-negative $\alpha1$ and $\alpha2$ AMPK were kindly provided by Dr J. Ha (Dept. of Molecular Biology, Kyung Hee University College of Medicine, Seoul, Korea). Adenoviruses containing either β-galactosidase (Ad-β-gal) or a mixture of dominant-negative $\alpha1$ AMPK and $\alpha2$ AMPK (Ad-DN-AMPK) were added to subconfluent C2C12 cells at a concentration of 50 plaque-forming

units per cell for 2 h at 37 °C in Dulbecco's modified Eagle's medium without serum, as described previously (32).

Immunoblotting Analysis—After stimulation for the indicated time, cells were washed once in ice-cold phosphate-buffered saline and lysed in a lysis buffer containing 20 mM Tris (pH 7.5), 150 mM NaCl, 1 mM EDTA, 1 mM EGTA, 1% Triton X-100, 2.5 mM sodium pyrophosphate, 1 mM β-glycerol phosphate, 1 mM Na$_3$VO$_4$, 1 μg/ml leupeptin, and 1 mM phenylmethylsulfonyl fluoride. The samples were centrifuged at 10,000 $\times$ g at 4 °C for 10 min, and the supernatants were collected. The proteins were separated on 10% SDS-polyacrylamide gels and transferred to Immobilon-P membranes (Millipore, Bedford, MA). The blots were incubated with 5% skim milk powder in TBST (10 mM Tris, pH 8.0, 150 mM NaCl, 0.05% Tween 20, also used for all incubation and washing steps) for 1 h at room temperature, and then incubated overnight at 4 °C with anti-phospho-Acetyl CoA polyclonal antibody (Upstate) or anti-acetyl-CoA polyclonal antibody (Upstate). After rinsing, the blots were incubated for 1 h with a 1:2,000 dilution of peroxidase-conjugated anti-rabbit IgG antibody. After washing three times, the signals were visualized with the Enhanced Chemiluminescence detection system (Amersham Biosciences).

Small Interfering RNA Construction—An appropriate siRNA sequence within the target melanocortin receptor mRNA sequence was chosen according to the manufacturer's software (provided by Ambion, Austin, TX). 5'-AAT GTG CTG GTT GTG GCC CCT GTC TC-3' and 5'-AAG GCT ATC ACA ACC AGC ACA CCT GTC TC-3' siRNA oligonucleotides for MC1R, 5'-AAC ACG TTC AAG GAG ATT CTC CCT GTC TC-3' and 5'-AAG AGA ATC TCC TTG AAC GTG CCT GTC TC-3' siRNA oligonucleotides for MC3R, and 5'-TCATTTGCCTCAT-CTCCATGT-3' and 5'-ACTGAGAGAGGAAGGCGTT T-3' siRNA oligonucleotides for MC5R were synthesized using a siRNA kit (Ambion) according to the manufacturer's instructions. C2C12 cells were plated in 6-well plates for RNA preparation and in 12-well plates for the palmitate oxidation assay. They were transfected at 70% confluency with 50 nM control siRNA or one of the melanocortin receptor siRNAs using Lipofectamine reagent (Invitrogen) according to the manufacturer's instructions. After transfection, cells were recovered in the regular growth medium for 48 h before inducing differentiation into myoblasts with differentiation medium. Effective RNA interference probes and their effective concentrations were determined based on their ability to inactivate cognate sequences. The effect of each siRNA was measured by quantitative RT-PCR gel analysis.

Statistical Analysis—Results are expressed as means $\pm$ S.E. Statistical analyses were performed using GraphPad Instat software (GraphPad Software, Inc.). All data were analyzed using the Student's *t* test or ANOVA.

RESULTS

Effect of α-MSH on FAO in Primary Muscle and C2C12 Cells—To investigate whether α-MSH regulates FAO in skeletal muscle, the activity of CPT-1, the rate-limiting enzyme in FAO, was measured. Mice were subcutaneously injected with 100 nM α-MSH, and CPT-1 activity in skeletal muscle was measured at 0, 0.5, 1, 3, and 5 h after α-MSH treatment. CPT-1
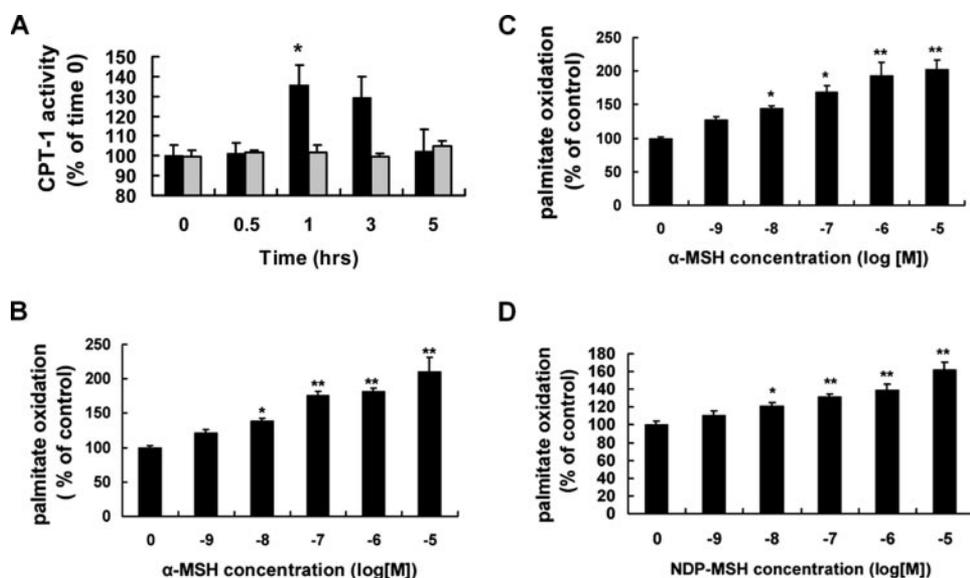
FIGURE 1. **Effect of α-MSH and NDP-MSH on FAO in skeletal muscle.** *A*, effect of α-MSH on CPT-1 activity in mouse skeletal muscle *in vivo*. 100 nM α-MSH was subcutaneously injected into C57BL/6J mice; CPT-1 activity in the skeletal muscle was measured at the indicated times. The value from each group is expressed as a percentage relative to that at 0 h (100%). *Bar* in *bold*, the α-MSH-administered group; *bar* in *gray*, placebo. *B* and *C*, a dose-dependent effect of α-MSH on palmitate oxidation in C2C12 cells (*B*) and primary culture mice skeletal muscle cells (*C*). Cells were treated with the indicated concentrations of α-MSH and palmitate oxidation was measured 2 h after treatment. *D*, effects of NDP-MSH on palmitate oxidation in C2C12 cells. C2C12 cells were treated with the indicated concentrations of NDP-MSH, and palmitate oxidation was measured after 2 h. Data are expressed as means ± S.E. of five independent experiments. *, $p < 0.05$; **, $p < 0.01$ *versus* control (ANOVA, Dunnett's test).
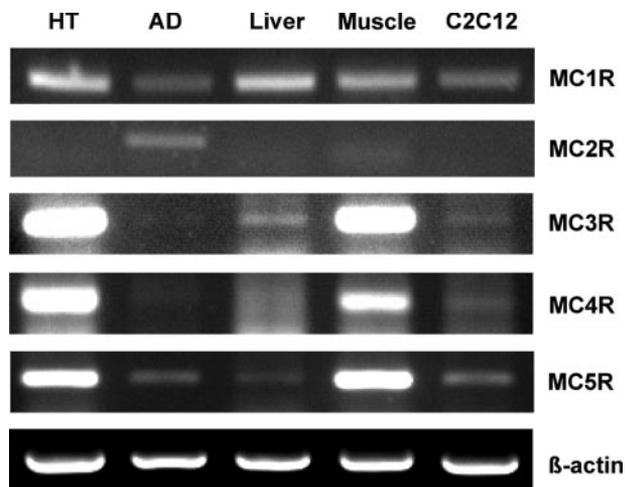

FIGURE 2. **RT-PCR analysis of MCR subtypes in mouse peripheral tissues and C2C12 cells.** Detection of mRNA corresponding to all five MCRs and β-actin in the hypothalamus (*HT*), adipose tissue (*AD*), liver, skeletal muscle, and C2C12 cells. The results are representative of five individual experiments.

activity increased significantly after treatment (36% increase at 1 h) and returned to the baseline level at 5 h (Fig. 1*A*). The effect of α-MSH on palmitate oxidation was also measured in C2C12 cells and primary culture muscle cells. In C2C12 cells, 10^{-8} M α-MSH induced a significant increase in palmitate oxidation (40% relative to control) and at 10^{-5} M α-MSH, palmitate oxidation increased to 210% (Fig. 1*B*). A similar dose-dependent effect was observed in primary muscle cells (Fig. 1*C*). NDP-MSH, another MCR agonist, also increased palmitate oxidation at concentrations ranging from 10^{-8} M to 10^{-5} M in C2C12 cells

(Fig. 1*D*), suggesting a functional role for MCRs in melanocortin-induced FAO in skeletal muscle.

MCR Subtypes Expressed in Skeletal Muscle and C2C12 Cells—To investigate the expression of the five MCR subtypes (MC1R, MC2R, MC3R, MC4R, and MC5R) in mouse peripheral tissues and C2C12 cells, RT-PCR was performed using primers specific to each subtype. The hypothalamus was used as a positive control. All subtypes, except MC2R, were detected at variable levels in skeletal muscle and C2C12 cells as well as adipose tissue and liver. Both MC1R and MC5R were diffusely expressed but most highly expressed in skeletal muscle (Fig. 2 and supplemental Fig. S1).

Identification of the MCR Subtype Mediating α-MSH-induced FAO in Skeletal Muscle—To clarify the functional subtype of MCR responsible for α-MSH-induced FAO in skeletal muscle, we treated C2C12 cells and primary muscle cells with several known agonists and antagonists. [Gln⁶]α-MSH-ND, which has an agonistic activity for only MC4R and MC3R, increased palmitate oxidation only at high concentrations (10^{-5} M) (Fig. 3*A*). SHU9119 is a potent, nonselective antagonist against both MC3R and MC4R; however, it is an agonist for both MC1R and MC5R (33). SHU9119 increased the effect of α-MSH-induced palmitate oxidation in C2C12 cells (Fig. 3*B*) and primary muscle cells (Fig. 3*C*). Moreover, SHU9119 alone increased palmitate oxidation in both cell lines (Fig. 3, *B* and *C*). JKC-363, a selective MC4R antagonist, slightly decreased α-MSH-induced palmitate oxidation, but not to a statistically significant degree (Fig. 3*D*).

Effects of siRNA against MCR on FAO—To further examine the role of MCRs on FAO in skeletal muscle, C2C12 cells were transfected with siRNAs designed to suppress expression of the MCR subtypes. Two days after transfection, the cells reached a confluent state, and the medium was exchanged with a differentiation medium containing 2% horse serum. After 3 days of differentiation, mRNA expression of three subtypes of MCR was suppressed by up to 60% for MC1R, 90% for MC3R, and 80% for MC5R compared with the control (Fig. 4*A*). α-MSH increased FAO in cells transfected with the control siRNA, and siRNA against either MC1R or MC3R failed to show any visible suppression of α-MSH induced FAO in these cells (Fig. 4*B*). However, no significant α-MSH-induced increase in FAO was observed in cells transfected with MC5R-specific siRNA (Fig. 4*B*).

Effects of α-MSH on AMPK Activity in C2C12 Cells and Primary Culture Muscle Cells—Activation of AMPK, a well known fuel-sensing enzyme present in skeletal muscle, increases FAO through the inhibition of acetyl-CoA carboxylase (24). To investigate the involvement of AMPK in α-MSH-induced FAO
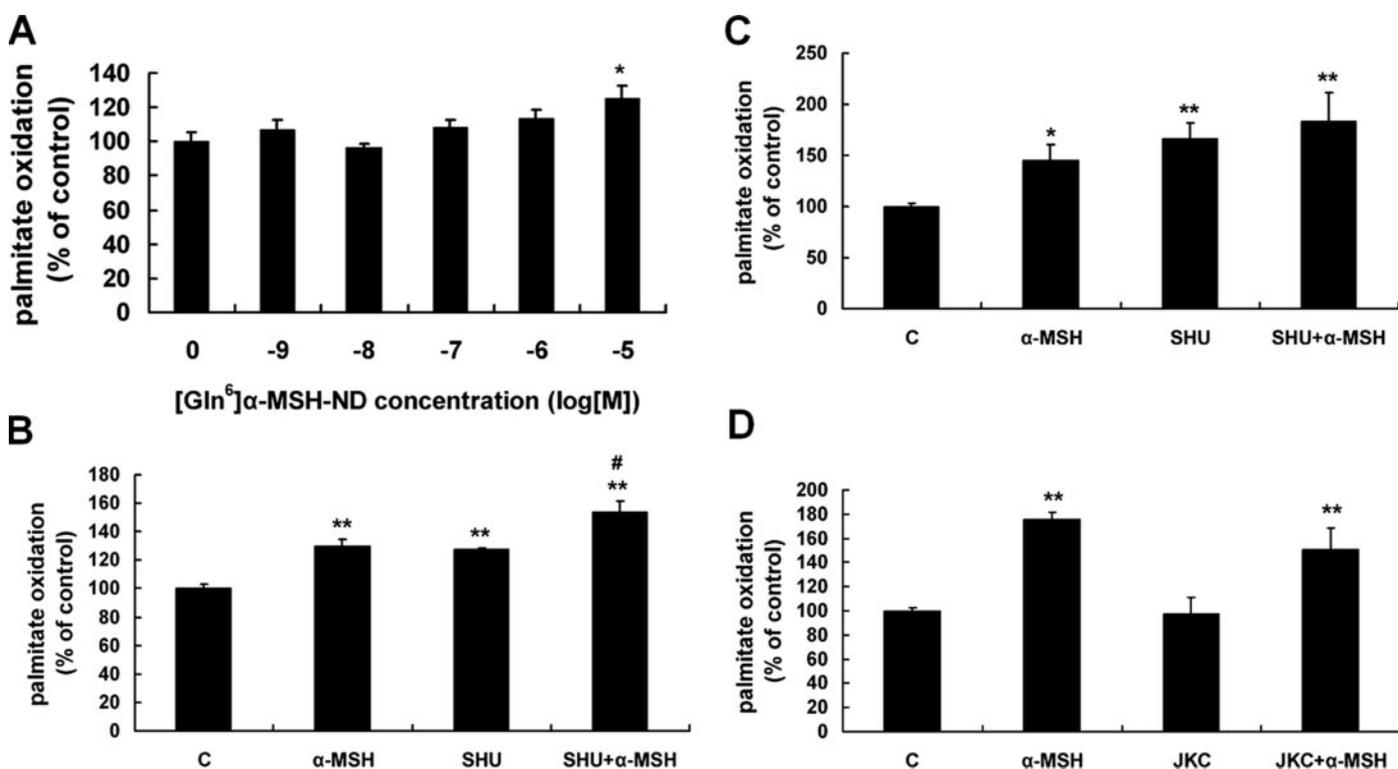
α-MSH Stimulates FAO in Skeletal Muscle

FIGURE 3. **Identification of the MCR subtype mediating α-MSH-induced FAO.** *A*, effects of [Gln[6]]α-MSH-ND on palmitate oxidation in C2C12 cells. C2C12 cells were treated with the indicated concentrations of [Gln[6]]α-MSH-ND, and palmitate oxidation was measured 2 h after treatment. Effects of SHU9119 (*B* and *C*) and JKC363 (*D*) on α-MSH-induced palmitate oxidation. Effect of SHU9119, an MC3R and MC4R antagonist and an MC1R and MC5R agonist, on palmitate oxidation in C2C12 cells (*B*) and primary culture muscle cells (*C*). C2C12 cells and primary culture muscle cells were pre-treated with 1 μM SHU9119 for 30 min, and 10 nM α-MSH was then added to the culture medium. Palmitate oxidation was measured 2 h later. *D*, effect of MC4R antagonist JKC363 on palmitate oxidation in C2C12 cells. Data are the means ± S.E. of five independent experiments. *, $p < 0.05$; **, $p < 0.01$ *versus* control (ANOVA, Dunnett's test); #, $p < 0.05$ *versus* control in the presence of the corresponding concentration of α-MSH (Student's *t* test).
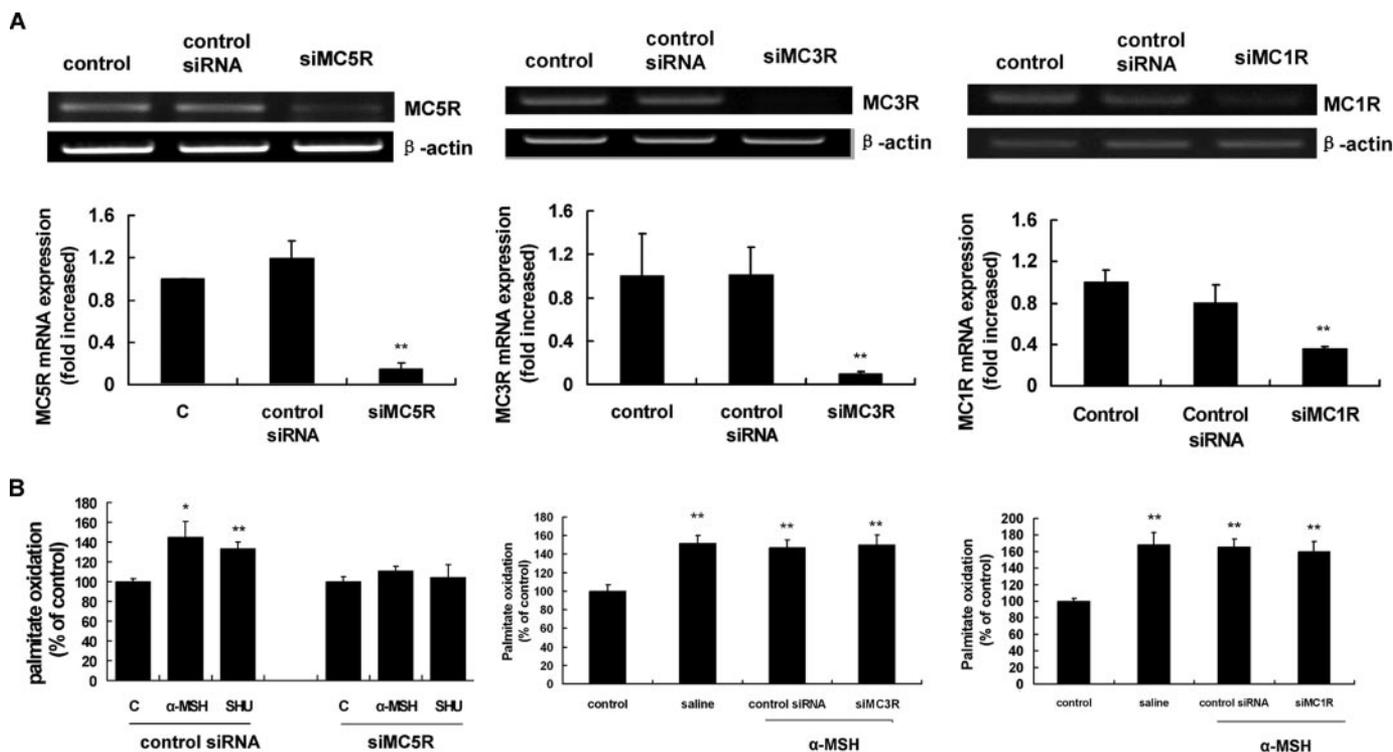

FIGURE 4. **Inhibition of endogenous MCR expression by siRNA.** *A*, results of RT-PCR showing a specific inhibition of each MCRs subtype (MC1R, MC3R, and MC5R) expression by siRNA. *Each bar* represents the mean and standards of error for three separate experiments. Each MCRs subtype densitometry values are normalized to β-actin. *B*, effect of siRNA against each MCRs subtype on α-MSH-induced palmitate oxidation. Data are the means ± S.E. of five independent experiments. *, $p < 0.05$; **, $p < 0.01$ *versus* control (ANOVA, Dunnett's test).
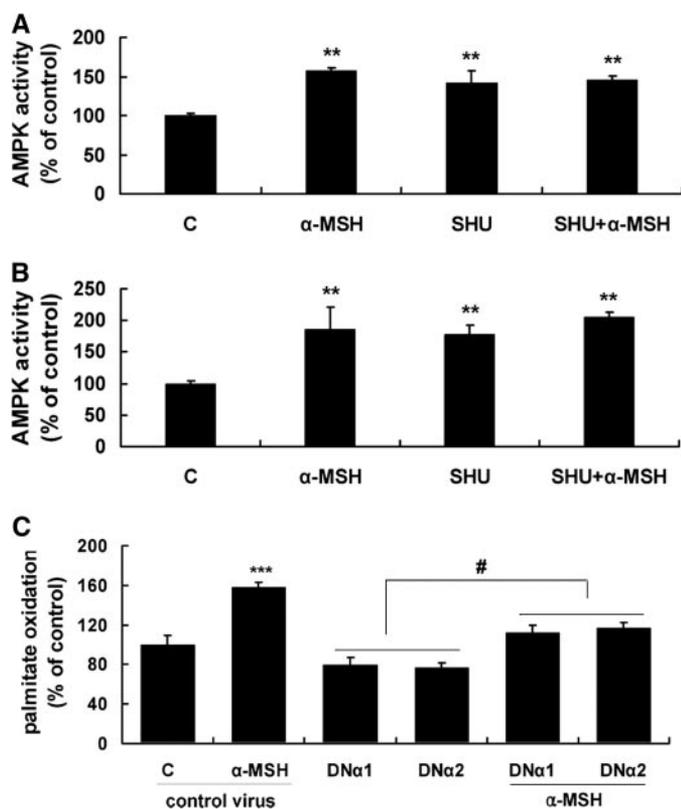
FIGURE 5. **Effect of α-MSH and SHU9119 on AMPK activity (*A* and *B*) and effect of dominant-negative AMPK on α-MSH-induced palmitate oxidation (*C*).** C2C12 cells (*A*) and primary culture muscle cells (*B*) were pre-treated with 1 μM SHU9119 for 30 min, and 10 nM α-MSH was then added to the culture medium. AMPK activity was measured 30 min later. Data are the means ± S.E. of four or five independent experiments. **, $p < 0.01$ *versus* control (ANOVA, Dunnett's test). After treatment with DN α1 and α2 AMPK for 2 h, palmitate oxidation was measured in the C2C12 cells measured (*C*). ***, $p < 0.001$ *versus* control; #, $p < 0.001$ (ANOVA, Dunnett's test).

in skeletal muscle, C2C12 cells and primary muscle cells were treated with α-MSH and SHU9119. AMPK activity was measured after 30 min. α-MSH treatment increased AMPK activity up to 56% in C2C12 cells and up to 86% in primary culture muscle cells. SHU9119 alone also increased AMPK activity, and co-treatment with α-MSH and SHU9119 did not reduce the effects of α-MSH on AMPK activity (Fig. 5, *A* and *B*). Dominant-negative AMPK partially blocked the α-MSH-induced increase in AMPK activity in C2C12 cells (Fig. 5*C*).

Involvement of cAMP and PKA in α-MSH-induced FAO— MCRs belong to the G-protein-coupled receptor family; they are all linked to cAMP generation via stimulatory G-proteins and adenylate cyclase. To investigate whether direct stimulation of the cAMP pathway could increase FAO, we measured palmitate oxidation and AMPK activity after treatment of C2C12 cells and primary culture muscle cells with two cAMP analogues, Bt$_2$cAMP and 8-Br-cAMP. Both analogues significantly increased palmitate oxidation (Fig. 6, *A* and *B*) and AMPK activity (Fig. 6, *C* and *D*) in both types of cells.

To further identify the role of cAMP in α-MSH-induced FAO in skeletal muscle, palmitate oxidation and AMPK activity were measured after treatment with the cAMP antagonist, (R_p)-cAMP, or the PKA inhibitor, H89, in C2C12 cells. Both (R_p)-cAMP and H89 effectively decreased α-MSH-induced palmi-

tate oxidation (Fig. 6*D*) and the activation of AMPK (Fig. 6*E*) in C2C12 cells, suggesting an important role for cAMP and the PKA activation pathway in α-MSH-induced FAO.

ACC Phosphorylation Is the Downstream Signal for α-MSH-induced FAO— AMPK activation increases FAO by inhibiting ACC activity and by decreasing the concentration of malonyl-CoA. ACCβ activity predominates in oxidative tissues, such as heart and skeletal muscle tissue. To further determine the role of AMPK and ACC on α-MSH-induced FAO, ACC phosphorylation was also examined in C2C12 cells. Treatment of C2C12 cells with 10^{-9} M α-MSH increased ACC phosphorylation (Fig. 7*A*). Meanwhile, SHU9119 treatment increased ACC phosphorylation (Fig. 7*B*). Treatment with a cAMP inhibitor or a PKA inhibitor suppressed α-MSH-induced ACC phosphorylation (Fig. 7*C*).

DISCUSSION

Our data demonstrate that α-MSH increased FAO in a dose-dependent manner in mouse skeletal muscle and C2C12 cells. In addition, we suggest that MC5R is the most probable subtype involved in inducing FAO in skeletal muscle, possibly via the cAMP-PKA-AMPK-ACC pathway.

Interest in the hypothalamic melanocortin system has increased dramatically during the past several years. The melanocortin pathway is important in the regulation of energy homeostasis (13), and there is little disagreement that the central melanocortin system is important for control of food intake and body weight (7, 8). However, the peripheral effects of melanocortins have rarely been studied, even though α-MSH has also been shown to have direct effects on several peripheral organ systems (17–19). Interestingly, peripheral administration of α-MSH to proopiomelanocortin null mice led to substantial weight loss, with melanocortins having a direct effect on adipocytes (13, 15). Forbes *et al.* (17) reported that α-MSH has a direct effect on lipid metabolism in adipocytes, perhaps through MC3R. In addition, there is increasing evidence for a peripheral action of melanocortins in the regulation of leptin expression in adipocytes (18, 19). However, the effects of melanocortins on skeletal muscle are not well understood, even though MCRs are expressed in skeletal muscle.

Peripheral injection of α-MSH significantly increased CPT-1 activity in mouse skeletal muscle (Fig. 1*A*) and α-MSH increased FAO in a dose-dependent manner in skeletal muscle cells (Fig. 1, *B* and *C*), suggesting that α-MSH regulates FAO through MCRs in the skeletal muscle.

Five subtypes of MCR have been cloned and characterized (16, 34–37). Among them, MC3R, MC4R, and MC5R are known to be expressed in both the central nervous system and in peripheral tissues. MC3R has been found in several nuclei of the hypothalamus, the pancreas, and the gastrointestinal tract; MC4R is found throughout the brain, in the sympathetic nervous system, and in muscle; and MC5R can be found in a broad spectrum of tissues, including the brain and skeletal muscle. Whereas MC5R is expressed in skeletal muscle (16), it was not known if other subtypes are also expressed. In this study, we demonstrated that four subtypes of MCRs (MC1R, MC3R, MC4R, and MC5R) were highly expressed at the mRNA level in mouse skeletal muscle cells and C2C12 cells. On the contrary,
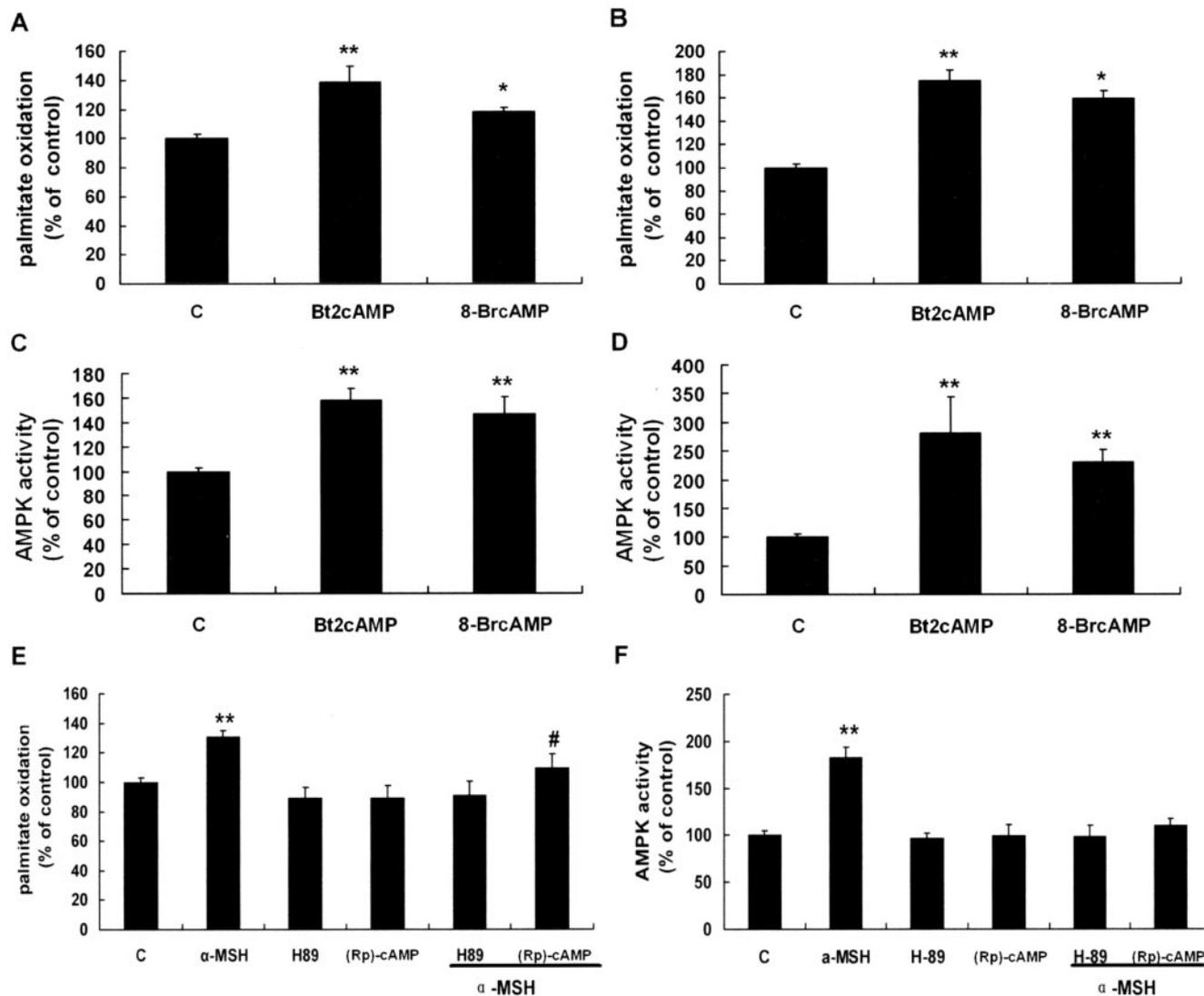
FIGURE 6. **Effects of the cAMP analogues Bt$_2$cAMP and 8-BrcAMP on palmitate oxidation and AMPK activity.** *A–D*, C2C12 cells (*A* and *C*) and primary culture muscle cells (*B* and *D*) were treated with the cAMP analogues Bt$_2$cAMP (50 μM) or 8-BrcAMP (100 μM). Palmitate oxidation (*A* and *B*) and AMPK activity (*C* and *D*) were measured 2.5 h after treatment, respectively. *E* and *F*, effect of PKA or cAMP inhibitor on α-MSH-induced palmitate oxidation and AMPK activity in C2C12 cells. After treatment of C2C12 cells with 10 μM H89 or 25 μM (R$_p$)-cAMP for 30 min, 10 nM α-MSH was added to the culture medium. Palmitate oxidation (*E*) and AMPK activity (*F*) were measured 30 min later. Data are the means $\pm$ S.E. of five independent experiments. *, $p < 0.05$; **, $p < 0.01$ *versus* control (ANOVA, Dunnett's test). #, $p < 0.05$, *versus* (R$_p$)-cAMP in the presence of the corresponding concentration of α-MSH (Student's *t* test).

extremely low levels of MCR mRNAs were observed in adipose tissue (Fig. 2).

Because mRNA expression does not necessarily represent protein expression or function, we performed serial experiments using MCR agonists and antagonists. Unexpectedly, [Glu^6]α-MSH-ND, which has ample potency for activation of both MC3R and MC4R, revealed very weak potency for the activation of FAO in C2C12 cells (only at 10^{-5} M, $p < 0.05$) (Fig. 3*A*) (38). These data suggest that neither MC3R nor MC4R is functioning in α-MSH induction of FAO in skeletal muscle. A potent and relatively selective MC4R antagonist, JKC-363, which is more potent than HS014, did not inhibit α-MSH-induced FAO (39, 40) (Fig. 3*D*). SHU 9119, which is both an MC3R and MC4R antagonist and an MC1R and MC5R agonist (33), enhanced the effect of α-MSH-induced FAO in skeletal muscle cells, and even SHU9119 alone increased FAO (Fig. 3, *B* and *C*). The above serial experiments using agonists and antag-

onists suggest that either MC1R or MC5R or both might mediate induction of FAO in skeletal muscle. siRNA against MCRs were used to identify the subtype mediating α-MSH-induced FAO in skeletal muscle. Only the siRNA against MC5R decreased FAO induced by either α-MSH or SHU9119 (Fig. 4*B*). Taken together, these data suggest that α-MSH induces FAO in skeletal muscle, primarily through direct interaction with MC5R. There have been few studies regarding the functional role of MC5R in the regulation of energy homeostasis. MC5R null mice showed water repulsion and reduced core body temperature after swimming (41). Only the Quebec Family Study has reported an MC5R association with obesity (42). Therefore, this is the first report suggesting a possible role for MC5R in mouse skeletal muscle energy metabolism.

MCRs are G-protein-coupled receptors; they are all coupled to adenylate cyclase via G-proteins. PKA activation stimulates the activity of CPT-1, a key enzyme in hepatocyte FAO (43).
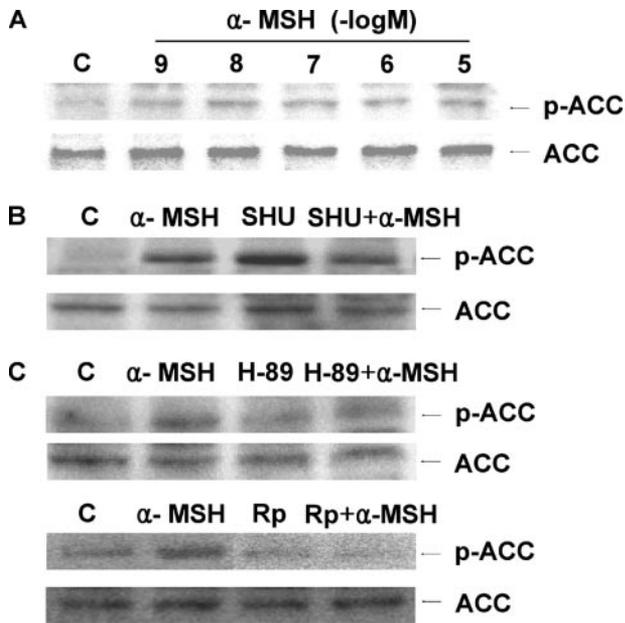
FIGURE 7. **α-MSH activates ACC in C2C12 cells.** *A*, Western blot analysis revealing a dose-dependent relationship between α-MSH and ACC phosphorylation. Cells were treated with the indicated concentration of α-MSH. Western blot was performed by using an anti-phospho-ACC antibody. To verify equivalent sample loading, an antibody against total ACC was also used. *B* and *C*, the effects of the melanocortin receptor antagonist, SHU9119, the PKA inhibitor, H-89, and the cAMP antagonist, (R_p)-cAMP, on ACC phosphorylation were also examined in C2C12 cells. Cells were pre-treated with SHU9119 (1 μM) (*B*), H89 (10 mM) (*C*), or (R_p)-cAMP (25 mM) (*C*) for 30 min and 10 nM α-MSH was then added for 30 min. Cells were analyzed by Western blot with anti-phospho-ACC antibody. The data, shown from one experiment, is representative of three or four similar experiments.

FIGURE 8. **Hypothetical pathway on the peripheral effect of α-MSH.** α-MSH-induced FAO seemed to be mediated through MC5R. The downstream involves cAMP-PKA activation. Then suppressing ACC activity by phosphorylation by unknown mechanism, resulted in the final activation of CPT-1 activity.

PKA activation is also required for leptin-induced FAO in aortic endothelial cells (44). In our study, two cAMP analogues increased FAO in both cell lines (Fig. 6, *A* and *B*); this was almost completely antagonized by treatment with either cAMP antagonist or PKA inhibitor (Fig. 6*E*). These results indicate that α-MSH-induced FAO may be mediated by cAMP-PKA activation in skeletal muscle.

AMPK is an intracellular energy sensor that has been implicated as a major regulator of FAO, glucose metabolism, and lipid metabolism in mammals. We observed that α-MSH-increased AMPK activity in skeletal muscle cells and dominant-negative AMPK partially abolished α-MSH-induced FAO (Fig. 5, *A–C*), indicating that AMPK activation is at least partially required. Recent studies have already revealed that AMPK activation increases FAO (22, 24) through the inhibition of ACC activity by phosphorylation in skeletal muscle. Even though phosphorylation of ACC by AMPK or PKA activation has been reported in both skeletal (45) and cardiac muscle (46), there are still some conflicts regarding PKA-induced ACC activation (45, 47). In 3T3L1 adipocytes, cAMP analogues lead to AMPK activation and maximal lipolytic activation (48). In this study, cAMP analogues increased AMPK activity (Fig. 6, *C* and *D*) in skeletal muscle cells with complete inhibition by a cAMP antagonist ((R_p)-cAMP) and a PKA inhibitor (Fig. 6*F*). These results suggest that activation of the cAMP-PKA signal transduction pathway could be important for AMPK activation in skeletal muscle cells. The lack of a consensus PKA phosphorylation site in AMPK (48) suggests that PKA regulates AMPK activity
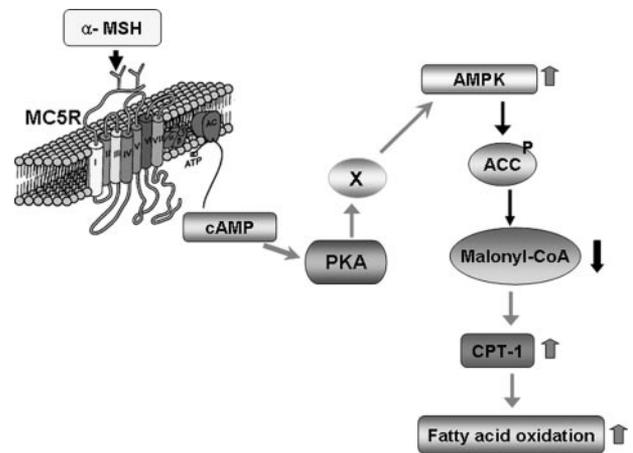
through an unknown mechanism. Treatment of C2C12 cells with α-MSH or cAMP analogues suppressed ACC activity by phosphorylation (Fig. 7), and the responses of ACC phosphorylation caused by SHU9119, H89, and (R_p)-cAMP were also similar to the changes in palmitate oxidation and AMPK activity. Taken together, these data suggest that PKA-AMPK activation, followed by ACC phosphorylation, plays a crucial role in α-MSH-induced FAO in skeletal muscle (Fig. 8).

Although classically considered as being of pituitary origin, proopiomelanocortin-derived peptides have been identified in a variety of peripheral tissues, such as the thyroid, pancreas, gastrointestinal tract, and placenta (49). α-MSH has also been found in circulating plasma (50). We have also found that the α-MSH significantly enhanced the 2-deoxyglucose uptake by insulin via pre-treating with α-MSH in C2C12 cells (supplemental Fig. S2). To delineate the direct peripheral effects of melanocortin, clear documentation of its role in other peripheral tissues and *in vivo* experiments addressing whole body lipid metabolism and insulin sensitivity are needed.

In conclusion, our study demonstrates that α-MSH regulates FAO in skeletal muscle through the activation of MCRs, mainly MC5R, and the activation of AMPK. Our data show possible involvement of the melanocortin system in the regulation of lipid metabolism in skeletal muscle, independent of its well known effects in the central nervous system. Furthermore, our findings may provide valuable insight regarding potential melanocortin analogues that could be used to improve insulin sensitivity by stimulating FAO in skeletal muscle.

REFERENCES

1. Kahn, B. B., and Flier, J. S. (2000) *J. Clin. Invest.* **106,** 473–481
2. Ferrannini, E. (1998) *Endocrinol. Rev.* **19,** 477–490
3. Pagliassotti, M. J., Pan, D., Prach, P., Koppenhafer, T., Storlien, L., and Hill, J. O. (1995) *Obes. Res.* **3,** 459–464
4. Pan, D. A., Lillioja, S., Kriketos, A. D., Milner, M. R., Baur, L. A., Bogradus, C., Jenkins, A. B., and Storlien, L. H. (1997) *Diabetes* **46,** 983–988

5. Goodpaster, B. H., Thaete, F. L., Simoneau, J. A., and Kelley, D. E. (1997) *Diabetes* **46,** 1579–1585

6. Simoneau, J. A., Colberg, S. R., Thaete, F. L., and Kelley, D. E. (1995) *FASEB J.* **9,** 273–278

7. Mizuno, T. M., Kleopoulos, S. P., Bergen, H. T., Roberts, J. L., Priest, C. A., and Mobbs, C. V. (1998) *Diabetes* **47,** 294–297

8. Fan, W., Boston, B., Kesterson, R., Hruby, V., and Cone, R. (1997) *Nature* **385,** 165–168

9. Grill, H. J., Ginsberg, A. B., Seeley, R. J., and Kaplan, J. M. (1998) *J. Neurosci.* **18,** 10128–10135

10. Huszar, D., Lynch, C. A., Fairchild-Huntress, V., Dunmore, J. H., Fand, Q., Berkemeier, L. R., Gu, W., Kesterson, R. A., Boston, B. A., Cone, R. D., Smith, F. J., Campfield, L. A., Burn, P., and Lee, F. (1997) *Cell* **88,** 131–141

11. Butler, A. A., Kesterson, R. A., Khong, K., Cullen, M. J., Pelleymounter, M. A., Dekoning, J., Baetscher, M., and Cone, R. D. (2000) *Endocrinology* **141,** 3518–3521

12. Chen, A. S., Marsh, D. J., Trumbauer, M. E., Frazier, E. G., Guan, X. M., Yu, H., Rosenblum, C. I., Vongs, A., Feng, Y., Cao, L., Metzger, J. M., Strack, A. M., Camacho, R. E., Mellin, T. N., Nunes, C. N., Min, W., Fisher, J., Gopal-Truter, S., MacIntyre, D. E., Chen, H. Y., and Van der Ploeg, L. H. (2000) *Nat. Genet.* **26,** 97–102

13. Yaswen, L., Diehl, N., Brennan, M. B., and Hochgeschwender, U. (1999) *Nat. Med.* **5,** 1066–1070

14. Cone, R. D. (1999) *Trends Endocrinol. Metab.* **10,** 211–216

15. Zemel, M. B., and Shi, H. (2000) *Nutr. Rev.* **58,** 177–180

16. Labbe, O., Desarnaud, F., Eggerickx, D., Vassart, G., and Parmentier, M. (1994) *Biochemistry* **33,** 4543–4549

17. Forbes, S., Bui, S., Robinson, B. R., Hochgeschwender, U., and Brennan, M. B. (2001) *Proc. Natl. Acad. Sci. U. S. A.* **98,** 4233–4237

18. Hoggard, N., Hunter, L., Duncan, J. S., and Rayner, D. V. (2004) *J. Mol. Endocrinol.* **32,** 145–153

19. Norman, D., Isidori, A. M., Frajese, V., Caprio, M., Chew, S. L., Grossman, A. B., Clark, A. J., Michaell Besser, G., and Fabbri, A. (2003) *Mol. Cell Endocrinol.* **200,** 99–109

20. Saggerson, D., Ghadiminejad, I., and Awan, M. (1992) *Adv. Enzyme. Regul.* **32,** 285–306

21. Winder, W. W., Arogyasami, J., Elayan, I. M., and Cartmill, D. (1990) *Am. J. Physiol.* **259,** E266–E271

22. Winder, W. W., Hardie, D. G., Elayan, I. M., and Cartmill, D. (1999) *Am. J. Physiol.* **277,** E1–E10

23. Hayashi, T., HIrshman, M. F., Fujii, N., Habinowski, S. A., Witters, L. A., and Goodyear, L. J. (2000) *Diabetes* **49,** 527–531

24. Ruderman, N. B., Saha, A. K., Vavvas, D., and Witters, L. A. (1999) *Am. J. Physiol.* **276,** E1–E18

25. Park, H., Kaushik, V., Constant, S., Prentki, M., Przybytkowski, E., Ruderman, N. B., and Saha, A. K. (2002) *J. Biol. Chem.* **277,** 32571–32577

26. Minokoshi, Y., Kim, Y. B., Peronl, O. D., Lee, G. K., Corinna, F., Muller, D. C., Carling, D., and Kahn, B. B. (2002) *Nature* **415,** 339–343

27. Daniels, M. P. (1990) *J. Cell Sci.* **97,** 615–626

28. Saggerson, E. D., and Carpenter, C. A. (1981) *FEBS Lett.* **129,** 229–232

29. Lowry, O. H., Rosebrough, N. J., Farr, A. L., and Randall, R. J. (1951) *J. Biol. Chem.* **193,** 265–275

30. Djouadi, F., Bonnefont, J. P., Munnich, A., and Bastin, J. (2003) *Mol. Genet. Metab.* **78,** 112–118

31. Kishi, K., Yuasa, T., Minami, A., Yamada, M., Hagi, A., Hayashi, H., Kemp, B. E., Witters, L. A., and Ebina, Y. (2000) *Biochem. Biophys. Res. Commun.* **276,** 16–22

32. Park, J. Y., Takahara, N., Gabriele, A., Chou, E., Naruse, K., Suzuma, K., Yamauchi, T., Ha, S. W., Meier, M., Rhodes, C. J., and King, G. L. (2000) *Diabetes* **49,** 1239–1248

33. Schioth, H. B., Muceniece, R., Mutulis, F., Bouifrouri, A. A., Mutule, I., and Wikberg, J. E. (1999) *Neuropeptides* **33,** 191–196

34. Chhajlani, V., and Wikberg, J. E. (1992) *FEBS Lett.* **309,** 417–420

35. Chhajlani, V., Muceniece, R., and Wikberg, J. E. (1993) *Biochem. Biophys. Res. Commun.* **195,** 866–973

36. Gantz, I., Konda, Y., Tashiro, T., Shimoto, Y., Miwa, H., Munzert, G., Watson, S. J., DelValle, J., and Yamada, T. (1993) *J. Biol. Chem.* **268,** 8246–8250

37. Gantz, I., Miwa, H., Konda, Y., Shimoto, Y., Tashiro, T., Watson, S. J., DelValle, J., and Yamada, T. (1993) *J. Biol. Chem.* **268,** 15174–15179

38. Lee, E. J., Lee, S. H., Jung, J. W., Lee, W., Kim, B. J., Park, K. W., Lim, S. K, Yoon, C. J., and Baik, J. H. (2001) *Eur. J. Biochem.* **268,** 582–591

39. Li, S. Z., Lee, J. H., Lee, W., Yoon, C. J., Baik, J. H., and Lim, S. K. (1999) *Eur. J. Biochem.* **265,** 430–440

40. Kask, A., Pahkla, R., Irs, A., Rago, L., Wikberg, J. S., and Schioth, H. B. (1999) *Neruo. Report.* **10,** 707–711

41. Chen, W., Kelly, M. A., Opitz-Araya, X., Thomas, R. E., Low, M. J., and Cone, R. D. (1997) *Cell* **91,** 789–798

42. Chagnon, Y. C., Chen, W. J., Perusse, L., Chagnon, M., Nadeau, A., Wilkison, W. O., and Bouchard, C. (1997) *Mol. Med.* **3,** 663–673

43. Velasco, G., Geelen, M. J., Gomezdel, P. T., and Guzman, M. (1998) *J. Biol. Chem.* **273,** 21497–21504

44. Yamagishi, S. I., Edelstein, D., Du, X. L., Kaneda, Y., Guzman, M., and Brownlee, M. (2001) *J. Biol. Chem.* **276,** 25096–25100

45. Winder, W., Wilson, H. A., Hardie, D. G., Rasmussen, B. B., Hutber, C. A., Call, G. B., Clayton, R. D., Conley, L. M., Yoon, S., and Zhou, B. (1997) *J. Appl. Physiol.* **82,** 219–225

46. Dyck, J. R., Kudo, N., Barr, A. J., Davies, S. P., Hardie, D. G., and Lopaschuk, G. D. (1999) *Eur. J. Biochem.* **262,** 184–190

47. Boone, A. N., Rodrigues, B., and Brownsey, R. W. (1999) *Biochem. J.* **341,** 347–354

48. Yin, W., Mu, J., and Birnbaum, M. J. (2003) *J. Biol. Chem.* **278,** 43074–43080

49. Smith, A. I., and Funder, J. W. (1988) *Endocr. Rev.* **9,** 159–179

50. Catania, A., and Lipton, J. M. (1993) *Endocr. Rev.* **14,** 564–576